# A cool look at the structural changes in kinesin motor domains

**Linda A. Amos[1,*] and Keiko Hirose[2]**

[1]MRC Laboratory of Molecular Biology, Cambridge, CB2 0QH, UK
[2]Research Institute for Cell Engineering, National Institute of Advanced Industrial Science and Technology (AIST), Tsukuba, Ibaraki 305-8562, Japan
*Author for correspondence (e-mail: laa@mrc-lmb.cam.ac.uk)

*Accepted 3 October 2007*
*Journal of Cell Science 120, 3919-3927 Published by The Company of Biologists 2007*
*doi:10.1242/jcs.016931*

## Summary

**Recently, several 3D images of kinesin-family motor domains interacting with microtubules have been obtained by analysis of electron microscope images of frozen hydrated complexes at much higher resolutions (9-12 Å) than in previous reports (15-30 Å). The high-resolution maps show a complex interaction interface between kinesin and tubulin, in which kinesin's switch II helix α4 is a central feature. Differences due to the presence of ADP, as compared with ATP analogues, support previously determined crystal structures of kinesins alone in suggesting that α4 is part of a pathway linking the nucleotide-binding site and the neck that connects to cargo. A 3D structure of the microtubule-bound Kar3 motor domain in a nucleotide-free state has revealed dramatic changes not yet reported for any crystal structure, including melting of the switch II helix, that may be part of the mechanism by which information is transmitted. A nucleotide-dependent movement of helix α6, first seen in crystal structures of Kif1a, appears to bring it into contact with tubulin and may provide another communication link. A microtubule-induced movement of loop L7 and a related distortion of the central β-sheet, detected only in the empty state, may also send a signal to the region of the motor core that interacts with the neck. Earlier images of a kinesin-1 dimer in the empty state, showing a close interaction between the two motor heads, can now be interpreted in terms of a communication route from the active site of the directly bound head via its central β-sheet to the tethered head.**

Key words: Cryo-electron microscopy, Image reconstruction, Microtubule motors

## Introduction

Kinesin motors use energy supplied by ATP hydrolysis to move cargo along microtubules (MTs) or, in some cases, to depolymerise these cytoskeletal filaments. All have very similar motor domains and appear to follow the same cycle of strong binding to tubulin when the nucleotide-binding pocket is empty or contains ATP and weak binding, leading to detachment, when ADP is bound (Fig. 1). Researchers in this field are interested in the conformational changes that accompany these chemical changes and the mechanisms that control the cycle. The three main functional regions of the motor domain that need to exchange information are the microtubule-binding interface, the nucleotide-binding site and the neck region that connects the motor domain to the cargo-binding domain of a full-length protein (Fig. 2). Mutagenesis and biochemical studies first indicated that a fairly extensive part of the surface is involved in tubulin binding (Fig. 2A,B,D,E show examples of motor domains as viewed from the MT). The nucleotide-binding pocket, on an adjacent part of the surface, is surrounded by several loops: the loop known as switch I lies close to the α- and β-phosphates of the bound nucleotide, whereas the P-loop and switch II loop are close to the position of the γ-phosphate that is lost when ATP is hydrolysed to ADP. The neck associates with another part of the surface of the motor domain, on the opposite side from the nucleotide-binding site. Plus-end-directed kinesins and minus-end-directed kinesins differ in having their neck regions connected to the C-terminal and N-terminal ends, respectively, of the motor domain. However, the necks emerge from a similar point in both cases (see Fig. 2C,F) and may be controlled in similar ways. Nevertheless, it is unclear in either case how binding to a MT stimulates the release of ADP, how ATP binding promotes neck movement or how neck movement leads to detachment of the motor domain from tubulin.

The database of protein crystal structures currently contains over 40 near-atomic models of motor domains from the kinesin superfamily. Although the list includes a variety of proteins from distant subgroups and some mutants, most structures are of motors in which ADP is bound to the nucleotide-binding pocket, since this is the default state for a free motor. In this state, the neck is usually disordered ('undocked') in the case of plus-end-directed motors (see Fig. 2D), whereas the N-terminal neck of a minus-end-directed motor is usually docked on to the surface of the motor domain (Fig. 2A). A few structures of plus-end-directed kinesin motors include bound analogues of ATP (Nitta et al., 2004; Kikkawa et al., 2001; Ogawa et al., 2004) and show interesting differences from the majority, including changes in the positions of the necks. A minority of the ADP-bound proteins (Sack et al., 1997; Kozielski et al., 1997; Turner et al., 2001; Yun et al., 2003) also appear to have crystallised with their necks in the 'wrong' conformations (Fig. 2B,E) but, overall, the structures seem consistent with the general idea that ADP and ATP binding

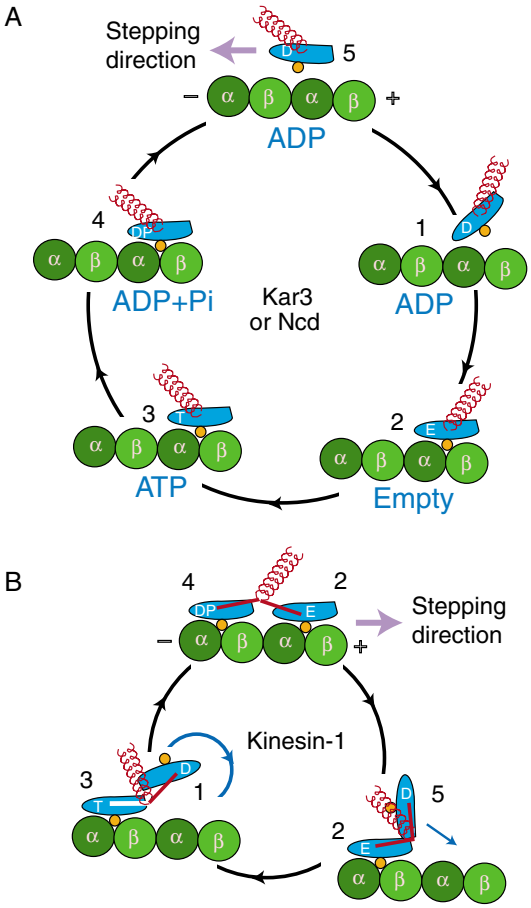


**Fig. 1.** Tentative schemes for conformational changes during ATPase cycles. (A) Motor acting as a monomer to contribute, in this case, to minus-end-directed movement. The motor domain is shown in cyan with the switch II helix in orange, the coiled-coil neck in red. The second head, thought to move passively with the coiled-coil, is not shown. The nucleotide bound to the motor is indicated at each stage in the cycle. (1) ADP-bound motor domain waiting to make contact with tubulin (part of one protofilament in a microtubule is shown as green subunits). The coiled-coil neck (red) is docked on to the motor domain. (2) Contact is made, ADP is released and the empty motor domain binds strongly to tubulin. (3) ATP binds to the nucleotide pocket. The coiled-coil, no longer docked on to the ATP-filled motor domain, is free to swing towards the MT minus end and allow other motors on the same cargo to search for new sites while this one remains attached. In an alternative model (Yun et al., 2003), the coiled-coil would be released by the loss of ADP and be free to move at stage 2. (4) ATP is hydrolysed to ADP and phosphate (Pi). (5) The motor domain detaches as phosphate is lost. Whilst the motor is unattached, the neck docks back on to the ADP-bound motor domain. (B) Processive dimer, whose two heads take turns in stepping towards the plus end of the MT (Vale et al., 1996; Schnitzer and Block, 1997; Hancock and Howard, 1998; Young et al., 1998; Carter and Cross, 2005; Hackney, 2007). White letters (E, D, T, DP) indicate the nucleotide states of individual heads. (1) The tethered, ADP-bound lead head is free to find a new binding site. It needs to swing around the junction with the neck-linker (red line) to bind to the same protofilament as the rear head. (2) ADP is released on contact and the empty lead head binds strongly. It must wait for the trailing head to finish ATP hydrolysis, release phosphate and detach (Klumpp et al., 2004), then wait to bind fresh ATP itself. The presence of the tethered head on the top of the leading head may provide the signal that allows ATP to bind. (3) ATP binds and the neck-linker is able to dock on to a site (shown as a white line) on the motor domain that helps to bias the binding of the new lead head to a site in the plus direction. (4) ATP is hydrolysed, making detachment possible once the lead head is firmly bound. (5) The detached head parks on top of the lead head while this head waits for ATP to bind (see main text and Fig. 6). In moving from position 4 to 5 and back to 1, the tethered heads must pass the coiled-coil on different sides during alternate steps, to avoid building up a twist.

each make a particular conformation of the neck more probable (Rice et al., 1999; Sindelar et al., 2002).

The crystal structures have led to a dominant model for how cargo may be moved relative to a plus-end-directed motor domain when a molecule of ATP enters the nucleotide-binding site (Figs 1, 2). Rice et al. (Rice et al., 1999) used a range of techniques, including low-resolution 3D electron microscopy (EM) of nanogold-labelled proteins, to show that the neck linker (which connects the neck with the rest of the motor domain) of kinesin is free to move when the motor domain is empty or bound to ADP but is bound to a site on the surface of the motor domain when ATP or an ATP analogue is present. Crystal structures of both kinesin-1 and Kif1a show that, when the neck linker is docked in position, there are also changes in the positions of the switch II helix α4 and nearby helix α5 (see Fig. 2D,E). It was proposed that these latter changes are caused by ATP binding and directly promote neck-linker docking, which, in turn, provides a force to move cargo towards the MT plus end (Rice et al., 1999). Although it has become clear that that neck-linker docking cannot provide enough energy to move the maximum load that dimeric kinesin has been observed to pull from one binding site to another, it is still thought likely that ATP-dependent neck linker docking provides some force as well as a directional bias. An equivalent model for Ncd (Endres et al., 2006) or Kar3 is even more problematical because any force towards the minus end would need to be generated by neck detachment (Fig. 1A and Fig. 2B).

Since there are no crystal structures of any kinesin family motor in the empty state, it is completely unclear how ADP is released and replaced by ATP. Nor is it known how neck movement or nucleotide hydrolysis within the motor domain control its binding to and detachment from tubulin. As yet, no crystallisation conditions have been found to induce crystals of a kinesin-tubulin complex. Electron microscopists have therefore been attempting to obtain equivalent information from high-resolution images of motor domains bound to MTs, which is possible when rapidly frozen unstained specimens are studied under cryo-EM conditions. The difficulty lies in collecting enough good images to average out the noise that masks the fine details. Recent achievements are two 10 Å maps of a monomeric motor domain (from mammalian Kif1a, a kinesin-3 motor) bound to β-adenylyl-imidodiphosphate (AMPPNP) or ADP (Kikkawa and Hirokawa, 2006), three 10-12 Å maps of a C-terminal motor domain (from yeast Kar3, a kinesin-14 motor), including a strongly bound empty state (Hirose et al., 2006), and a 9 Å map of a single motor domain of human conventional kinesin (kinesin-1, a processive dimeric motor) (Sindelar and Downing, 2007). At these levels of resolution, it is possible to detect features such as α-helices and

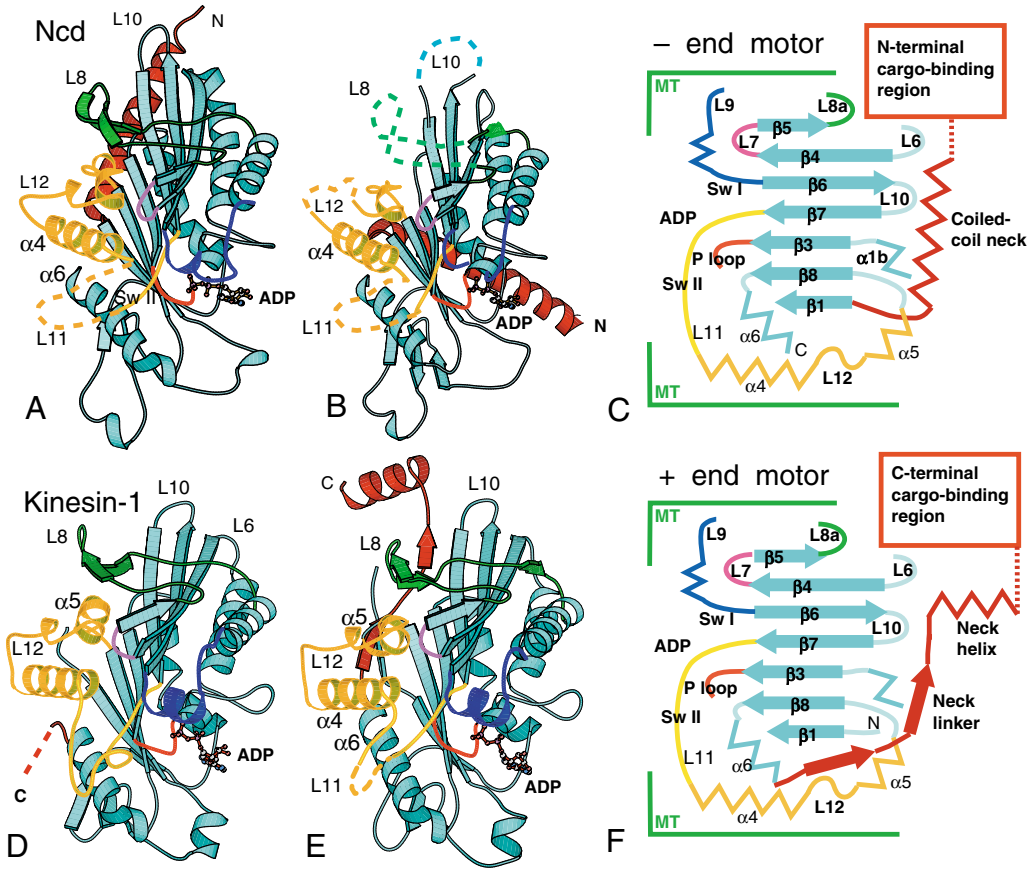


**Fig. 2.** Atomic structures of a C-terminal and an N-terminal kinesin family motor domain. (A,B) Crystal structures, represented in cartoon format, of the motor domain of Ncd, a minus-end-directed kinesin-14. In A, showing the conformation thought to predominate in the normal soluble ADP-filled state, the N-terminal neck helix (dark red) is docked against the edge of the central β sheet of the motor domain (Sablin et al., 1998; Kozielski et al., 1999); under the conditions used to crystallise the structure shown in B (Yun et al., 2003), the neck is not docked and has swung down around a hinge at its base. Yun et al. suggested that this conformation represents the empty state; alternatively, it may resemble an ATP-bound state, as suggested by Endres et al. (Endres et al., 2006). The crystal structure does not show any obvious changes that would indicate how the movement might be controlled, except that the adjacent loops are disordered. The switch II region (including L11, α4, L12 and α5) is coloured in gold, switch I in blue and loop L8 in green. The way these two conformations may produce movement along a MT is shown in Fig. 1A. (C) Simplified scheme of the polypeptide, with important loops and helices coloured as in A and B. (D,E) Crystal structures of the motor domain of kinesin-1. The C-terminal neck is not in a fixed position in the ADP state [D (Kull et al., 1996)]; however, the buffer conditions used for E (Sack et al., 1997; Sindelar et al., 2002) caused it to dock against the motor domain in a way that is thought to occur in the ATP-bound state ('ATP-like'). There are also some differences in the adjacent elements, loop L12, helix α5 and the switch II helix α4, that connect to the nucleotide-binding site. As indicated in Fig. 3C, crystal structures of Kif1a with ATP analogues bound show similar changes (Nitta et al., 2004). (F) F shows a schematic view of a plus-end-directed motor domain and its neck. PDB codes 1CZ7, 1N6M, 1BG2, 2KIN.

compare their positions with those in crystal structures by superimposing the latter as closely as possible on to the protein-density maps obtained by EM (as in Figs 3 and 4).

## Images of kinesin-family motor domains bound to microtubules

The general orientation of motor domains on MTs has been clear for many years from mutagenesis and biochemical studies (Woehlke et al., 1997; Alonso et al., 1998). The recent high-resolution EM maps of different kinesin motors all show basically the same orientation (Kikkawa and Hirokawa, 2006; Hirose et al., 2006; Sindelar and Downing, 2007): there is general agreement that the switch-II-helix α4 is situated in the groove between α- and β-tubulin (see Fig. 5), whereas loop L8 and the loops at either end of α4 (L11 and L12) interact directly with tubulin (Fig. 3A,B and Fig. 4A). There is less agreement about structural changes that take place throughout the cycle. The currently available 3D data that show nucleotide-dependent structural changes are summarised in Table 1 and are described below in more detail. Tightly bound ATP-like states are most easily studied, by use of non-hydrolysable analogues such as AMPPNP to obtain MTs fully decorated with motor domains. Empty states are also usually tightly bound and occur when all free nucleotides are removed. It is most difficult to obtain full decoration in the weakly attached ADP-bound state but this may be achieved by a high motor protein concentration and low ionic strength.

## Differences between ADP- and ATP-bound states

Images at 10 Å resolution obtained by Kikkawa and Hirokawa (Kikkawa and Hirokawa, 2006) show changes between ADP-bound and AMPPNP-bound Kif1a motor domains attached to

tubulin that mostly resemble those in the equivalent crystal structures of Kif1a alone. Apart from the movement of the neck linker, the most striking difference between the ADP and ATP-like states, a 20° rotation of the core domain relative to α4, is also evident in the EM maps (Fig. 3B). A much smaller shift seen in different crystal structures of conventional kinesin-1 alone (Fig. 2D,E) also correlates with the position of the neck linker (Sindelar et al., 2002) but no nucleotide-dependent rotation was evident in EM maps of kinesin-1 motor domains bound to MTs (Rice et al., 1999). Moreover, the bound motor domains of ADP-filled dimeric kinesin molecules attached to MTs were, apparently, able to rotate freely through a large angle (30-40°) in the opposite direction, to relieve a clash between the coiled-coil stalk and the MT (Hirose et al., 1999) (see also Fig. 6C). No clear rotation, nucleotide-dependent or otherwise, has yet been detected in other plus-end-directed motors, such as Unc104 (Al-Bassam et al., 2003) and Cenp-E [reconstructed to 15 Å resolution (Neumann et al., 2006)], or in minus-end-directed (kinesin-14 family) motors, such as Kar3 (Hirose et al., 2006) or Ncd dimers [for which it would have been apparent from the position of the tethered head (Hirose et al., 1998; Wendt et al., 2002; Endres et al., 2006)]. There is thus no evidence that a large-scale rotation of the motor core is a fundamental feature of communication between the enzymatic site and the cargo-binding domain. Instead the rotation of the Kif1a motor core may be a side-effect of more fundamental changes in α4 during nucleotide exchange (see below).

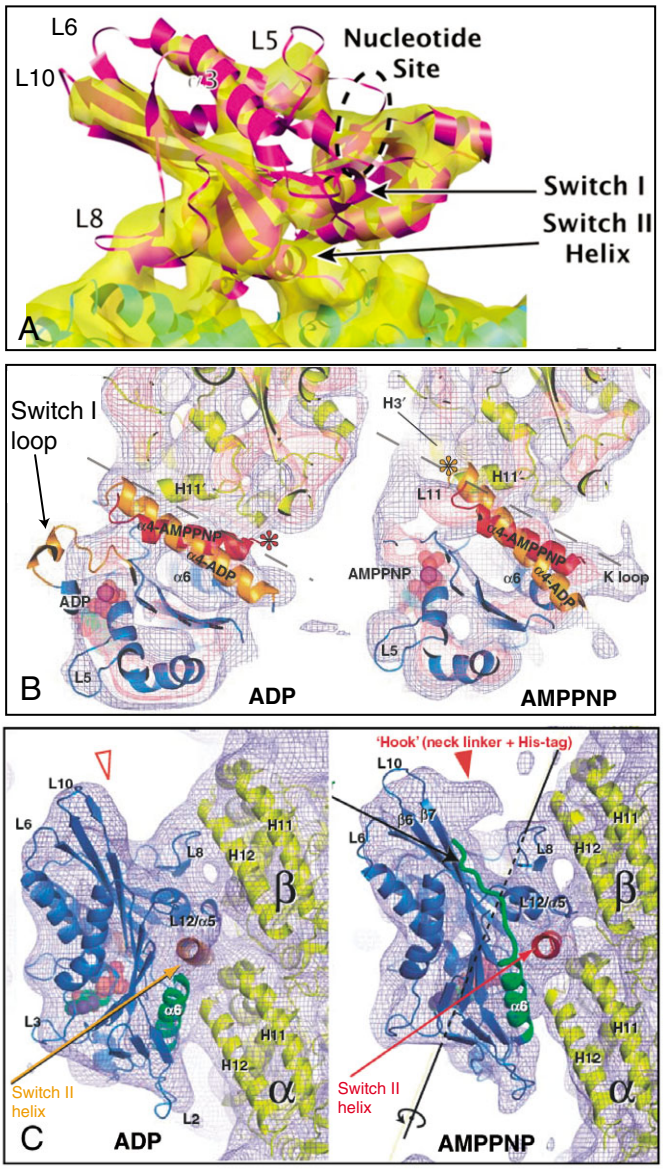


**Fig. 3.** High-resolution EM maps of plus-end-directed motors bound to microtubules. (A) Surface representation showing kinesin-1 bound to a MT (Sindelar and Downing, 2007). The secondary structures (superimposed in cartoon form) from kinesin-ADP crystals (PDB code 1BG2) (Kull et al., 1996) dock rather precisely into the EM map. (B,C) Sections through EM maps (density represented as a grey net) of the Kif1a motor domain attached to tubulin in two nucleotide states (ADP-bound and AMPPNP-bound) with corresponding crystal structures superimposed (from Kikkawa and Hirokawa, 2006). The view from the MT plus end (B) compares two positions of helix α4 (yellow for the ADP-bound state, red for the AMPPNP-bound state) relative to the motor core. In the side view (C), changes in helix α6 (green) are indicated, as well as changes indicating the reduced mobility of the neck linker when AMPPNP is bound.

An unexpected feature of the EM images of Kif1a is that α4 and its attendant loops, L11 and L12, appear as a longer rod of density in the map of the AMPPNP state, even though α4 is shorter in the AMPPNP crystal structure (see Fig. 3B). Also, the switch I loop of the superimposed crystal structure lies outside the strong density of the EM map of the ADP state, which suggests that this loop moves closer to the MT. However, the crystal structures and EM maps agree in showing the nucleotide-binding pocket of Kif1a is more open in the ADP state than in the AMPPNP state. The same is true for Kar3. The combined results from Kif1a and Kar3 clearly indicate that there is an important communication route extending via α4 and loops L11 and L12, from the nucleotide-binding pocket to the base of either the C-terminal neck-linker of a plus-end-directed kinesin (see Fig. 2D-F) or the N-terminal neck of a minus-end-directed motor (see Fig. 2A-C). As mentioned above, it has been proposed to carry the signal, during nucleotide exchange, from the active site to the neck. Alternatively or additionally, it may transmit a message in the opposite direction, from the cargo-binding region to the MT-binding region, to signal that the neck linker is docked, that there is currently no rearwards force and that the motor domain can safely detach from the MT (Rob Cross, personal communication). In myosin, the equivalent switch II helix is also thought to be a major route of communication (Vale and Milligan, 2000). However, it connects the nucleotide-binding site to the converter domain that controls the motion of the lever arm directly, rather than via the track-binding site as in kinesin.

Another very significant difference between the two states is in the position of helix α6 (shown green in Fig. 3C), which moves closer to tubulin when an ATP analogue is bound. The maps of the minus-end-directed Kar3 suggest similar changes may occur there (Fig. 4E). Since the P-loop is situated directly below α6 (Fig. 2), a movement of α6 in either plus-end-directed or minus-end-directed motor domains could transmit a signal directly from the nucleotide-binding pocket to the neck-binding side of the motor domain and thus contribute to the docking or undocking of the neck. Such a signal might operate in addition to that proposed to act via the switch II region.

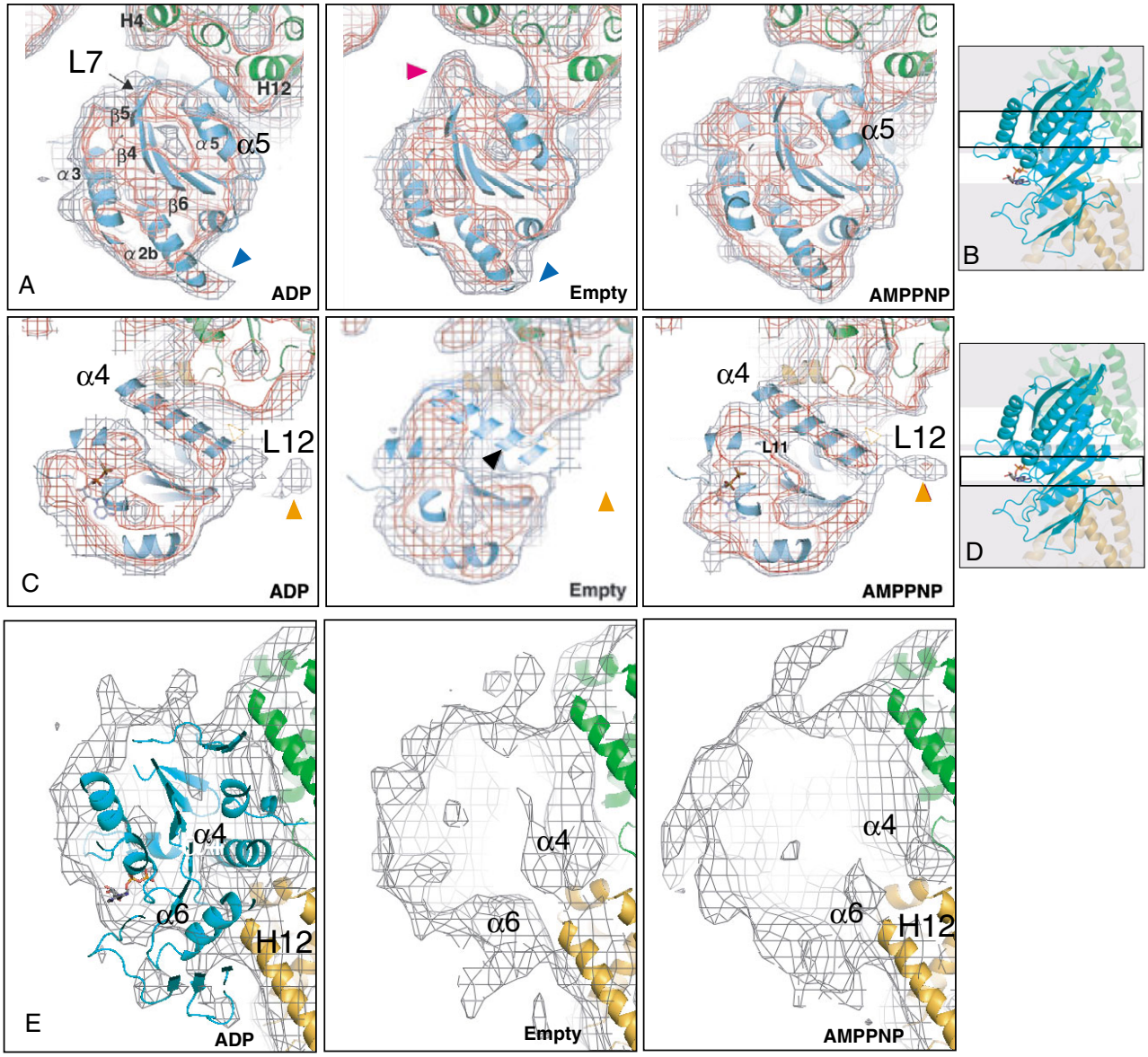


**Fig. 4.** High-resolution EM maps of Kar3 motor domains bound to microtubules. (A,C) Sections at two different levels through maps of the Kar3 motor domain in three different nucleotide states (ADP-bound, empty or AMPPNP-bound) with the Kar3-ADP crystal structure (cyan α-helices and β-strands; PDB code 1F9T) (Yun et al., 2001) docked into the EM density (represented by red and grey nets) (Hirose et al., 2006). The view is from the MT plus end and the positions of sections A and C within the 3D structure are indicated in panels B,D. Parts of α- and β-tubulin are included, with the crystal structures (PDB code 1JFF) (Löwe et al., 2001) shown in gold and green. The red arrowhead in A indicates a feature in the EM density of the nucleotide-free Kar3 that is absent from either of the nucleotide-bound motors and may be loop L7 in a new position. Blue arrowheads in A indicate the point at the top of the motor domain that is retracted in the empty structure. A also shows a movement of helix α5, which is closer to tubulin in the empty and AMPPNP-bound states. A black arrowhead in C indicates a marked loss of density from the region occupied by the switch-II-helix α4 in the other structures. Orange arrowheads point to the L12 loop that also disappears in the empty structure. (E) Sections though the three maps viewed from the side. There are changes in the position of helix α6 relative to switch II helix α4 and helix H12 of α-tubulin but, with only one Kar3 crystal structure available, we cannot be certain that the movement is the same as in Kif1a (Fig. 3C).

## Differences between nucleotide-bound states and the empty state

Both ends of the switch-II-helix α4 have been observed to vary in length in different crystal structures of Kif1a and it has been proposed by Nitta et al. (Nitta et al., 2004) that binding to tubulin is initiated by loop L12 at the C-terminal end of the helix, whereas nucleotide exchange causes loop L11 at the other end to bind more strongly and L12 more weakly. It was unclear how changes at one end of the helix could affect the other end but now the 3D image of the MT-bound empty state of Kar3 (Hirose et al., 2006) suggests that most of the helix melts during nucleotide exchange (Fig. 4C); its C-terminal half and loop L12 are no longer distinguishable from tubulin density. This dramatic loss of secondary structure is

**Table 1. Cryo-EM images of motor domains bound to microtubules and related structural data**

| Kinesin structure | ADP state | Empty state | AMPPNP/ATP-like state | References |
|---|---|---|---|---|
| Minus-end-directed monomer | Kar3 NTP pocket 'half-open'; switch II helix α4 fairly long. | Kar3 NTP pocket wide open; α4 melted on to MT together with L11 and L12; L7 loop closer to MT, β-sheet distorted by tight binding. | Kar3 NTP pocket closed; α4 partially reformed. | Hirose et al., 2006[1] |
| Minus-end-directed dimer | Ncd second head 'tethered'. Neck docked. | Ncd second head 'tethered'. Neck docked or undocked. | Ncd second head 'tethered'. Neck undocked. | Hirose et al., 1998[4]; Sosa et al., 1997; Wendt et al., 2002; Endres et al., 2006[5]; Sablin et al., 1998[12]; Kozielski et al., 1999[13]; Yun et al., 2003[14] |
| Plus-end-directed monomer | Kif1a NTP pocket 'open'; α4 in 'down' position; C-terminal neck undocked; α4 extended into L11, weakening its interaction with MT. Labelled kinesin neck undocked. | Conventional kinesin switch II helix α4 extended into L11; weak interaction with MT – but see text. Kinesin neck undocked. | Kif1a NTP pocket closed; α4 short and rotated to 'up' position; core domain rotated relative to MT; L11 interacts with MT; C-terminal neck docked. Cenp-E and Unc104 neck linkers docked, little or no rotation of core domains. Kinesin neck docked. | Kikkawa and Hirokawa, 2006[2]; Sindelar and Downing, 2007[3]; Rice et al., 1999[6]; Neumann et al., 2006[7]; Al-Bassam et al., 2003[8]; Kikkawa et al., 2001; Nitta et al., 2004[15] |
| Plus-end-directed dimer | Two kinesin heads interact weakly | Kinesin second head parked firmly on first head. | Kinesin second head tethered but fairly free. | Hirose et al., 1996; Hirose et al.,1999; Cross et al., 2000[9]; Arnal and Wade, 1998[10]; Fig. 4C within Hoenger et al., 1998[11]; Kozielski et al., 1997[16] |

[1-3]References referring to high-resolution EM structures; [4-11]references referring to lower-resolution structures; [12-16]references referring to crystal structures.

compensated by the intimate interaction with tubulin and it is probably significant that, in the absence of MTs, kinesin proteins without nucleotide tend to denature. The melting of α4 coincides with ADP loss but its secondary structure is restored when ATP binds. We suggest that this refolding represents the beginning of the process of detachment, which is completed after ATP hydrolysis and Pi release.

Another large change observed in the MT-bound empty state of Kar3 is the movement of the region that includes loop L7. This loop was originally thought to be a part of the MT-binding region (Woehlke et al., 1997), but superimposing the crystal structures on to previous EM maps showed some distance between L7 and tubulin. The new Kar3 map in the empty state shows movement of this loop toward helix H4 of β-tubulin (Fig. 4A). Since L7 interacts with the switch II loop in crystal structures, binding of the MT to L7 and the switch II helix may move the loops surrounding the nucleotide-binding pocket and trigger release of ADP.

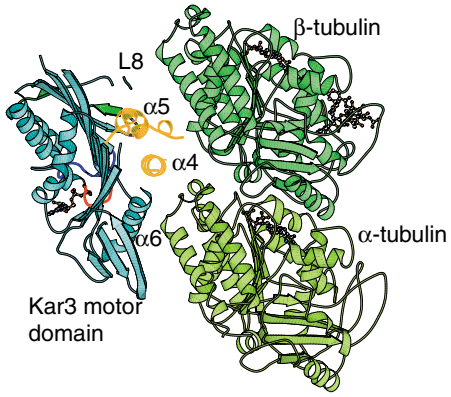


**Fig. 5.** Kar3 bound to tubulin. Binding orientation of Kar3 motor domain on αβ-tubulin, based on docking crystal structures into the EM maps (see Fig. 4). Different parts of Kar3 are coloured as in Fig. 2, including the switch II region in yellow. Loop L8 and helix α6 are also part of the interface with tubulin. Similar interactions for kinesin and Kif1a are apparent in Fig. 3A,C.

A 3D map of conventional kinesin bound to a MT without added nucleotide (Sindelar and Downing, 2007) has the highest resolution obtained so far (see Fig. 3A) – a remarkable achievement given that these authors found the motors to be so weakly bound that they had difficulty in keeping them attached while preparing EM grids. In contrast to the nucleotide-free Kar3 map, the kinesin-1 map shows an elongated switch II helix and no movement of L7. This could be owing to a difference between the minus-end-directed and plus-end-directed motors but it is more likely that these two structures are in different states. The reason for the weak binding to MTs reported by Sindelar and Downing is unclear, because an empty motor is normally strongly bound. The only difference in the conditions was that, during apyrase treatment to remove ATP and ADP, they exposed the motor domains to GTP, which would have bound to the kinesin nucleotide pocket (Cohn et al., 1989) and have been hydrolysed to GDP. It is possible, though unexpected, that this bound GDP was not lost during the subsequent centrifugation through a nucleotide-free sucrose cushion and dilution with a nucleotide-free buffer. No nucleotide is detectable in the 3D map (Fig. 3A) but the resolution is too low to be sure of its absence.

When loop L7 moves in Kar3, the central β-sheet, which is associated with this loop, should also change structure and this appears to affect the 'point' at the top of the sheet (Loop L10 in Fig. 2A, blue arrowheads in Fig. 4A). These changes reveal a further communication route: between the MT-binding loops and the neck. In the case of Kar3, changes in the β-sheet may

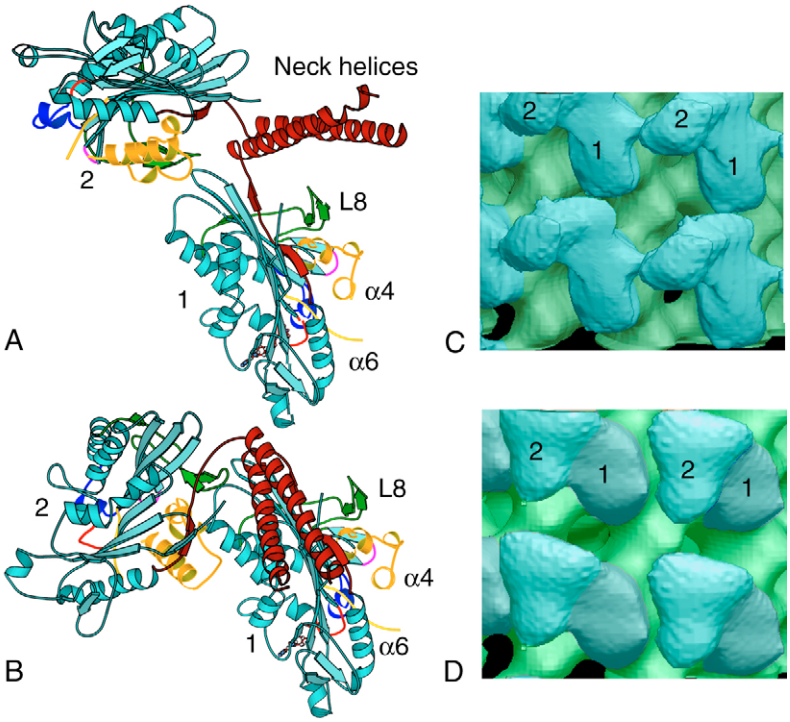


**Fig. 6.** Models of kinesin-1 dimers bound to tubulin. (A) Crystal structure of the rat kinesin-1 dimer (PDB code 3KIN) (Kozielski et al., 1997) with head 1 in the same orientation as the Kar3 head in Fig. 5. Note that the coiled-coil would clash with tubulin unless it moves from its position in the crystal structure. When MT were decorated with ADP-bound dimers (see C), a rotation of the whole motor domain apparently relieved the clash (Hirose et al., 1999). (B) The kinesin dimer crystal structure with the heads reoriented relative to each other to allow them both to dock into the EM map in D, with head 1 as the directly-bound head. The movement of head 2 is likely to have resulted from conformational changes in head 1 but the details are unknown. The coiled-coil (dark red) is shown as having shifted with head 2, though it was not detectable in D and was probably free to move anywhere. (C,D) Parts of the outer surfaces of low-resolution EM maps of kinesin-1 dimer bound in the ADP-bound and empty states to MTs (Hirose et al., 1999). Directly bound heads (1) and tethered heads (2) (both coloured here in cyan) can be identified. The MT is coloured green.

lead to displacement of the neck from the site to which it docks in the ADP state. Similar changes in the β-sheet of kinesin-1 would be expected to have a different effect because of the difference in the necks (Fig. 2).

## Lower-resolution images of dimeric motors

Although there is not yet any high-resolution image showing changes in the β-sheet of a plus-end-directed kinesin, there is some evidence from low-resolution images of kinesin dimers that the conformation of the core domain of kinesin-1 in the empty state is significantly different from that of the nucleotide-bound states. Whereas heads of a nucleotide-filled kinesin dimer appear either as separate entities or loosely associated (e.g. Fig. 6C), in conformations likely to be similar to the rat kinesin dimer crystal structure (Fig. 6A), in the nucleotide-free state the tethered head appears to be closely associated with the directly bound head (Fig. 6D). As detailed in Table 1, the empty state is the only one for which images of dimeric kinesin from different research groups have all shown density corresponding to a specifically bound tethered head[1]. Relative to the crystal structure of dimeric kinesin (Fig. 6A), the tethered head in Fig. 6D appears to tilt downwards (as modeled in Fig. 6B), which may be a consequence of structural changes associated with the proposed distortion of the central β-sheet.

Details of the interactions between the two heads have been clarified by recent studies of kinesin-tubulin complexes. Alonso et al. have shown that the 'gate' allowing ADP to be released from kinesin, which is closed in the absence of tubulin, can be opened by soluble tubulin and not just by assembled MTs (Alonso et al., 2007). An interaction with soluble tubulin had previously been observed in the case of the specialised members of the kinesin family that act as MT depolymerisers (Moores and Milligan, 2006) but now it is clear that conventional kinesin-1 behaves similarly. Moreover, the interaction with tubulin, like that with MTs, releases ADP from only one of the heads of a kinesin dimer and the other must wait for the first to bind ATP before it can follow suit. As long as the first head is empty, it seems to shield the second head from interacting with tubulin and releasing its ADP. These results undermine models in which the so-called waiting state relies on a signal transmitted by tension produced by having both heads bound simultaneously to the MT lattice. Instead, they strongly support the idea of a direct interaction between the heads and indicate that the nucleotide-free state observed by cryo-EM corresponds to an actual stage in the cycle of processive movement (Fig. 1B; bound head at stage 2 and tethered head at stage 5). Combining these observations with the new results obtained by high-resolution EM thus leads to the idea that changes in the β-sheet of kinesin-1 may provide a parking site for the tethered head on the top of the currently active head during the time spent waiting for ATP to bind (the 'dwell time') and then dislodge it when ATP binds, so that it is free to bind to the next site on the MT. Parking of the tethered head on top of the directly bound head could also send a signal in the opposite direction to allow ATP to bind.

[1]The same second-head arrangement of dimeric kinesin decorating MTs in the absence of nucleotide was reported independently by Arnal and Wade (Arnal and Wade, 1998), and even an image published by Hoenger et al. (Hoenger et al., 1998), who reported in their text that they saw only one head, shows a similar, though slightly smaller, feature. The reduced apparent size is easily explained by blurring owing to the greater mobility of a domain not in direct contact with the MT. To see equal-sized heads, we selected images with the best-ordered second heads for inclusion in the averaged data. Proponents of the model in which the dwell time (see main text) is spent with both heads simultaneously bound to adjacent sites on the MT (Hoenger et al., 1998; Hoenger et al., 2000; Hackney, 2007) have suggested that the tethered heads seen in our reconstructed images belong to a non-specifically bound extra layer of molecules. This does appear to be a reasonable explanation for some reconstructed images (Hoenger et al., 2000) (K.H. and L.A.A., unpublished) obtained from poorly soluble motor-domain constructs, when the decorated MTs appear thickly encrusted with non-specifically bound molecules. In such cases, molecules in a second layer (and sometimes even a third layer) occupy the holes in the underlying layer so that each contacts 2-4 different heads in that layer. This is in marked contrast to specifically bound kinesin dimers, whose second heads each make contact with only one directly bound head.

## Conclusion/Perspectives

High-resolution images of kinesin-family motor domains bound to MTs under conditions that mimic specific stages in the nucleotide hydrolysis cycle clearly support the idea that the switch II helix is the central structure involved in MT binding and is in close communication with the nucleotide-binding pocket. For both plus-end- and minus-end-directed motors, there are changes at each end of this helix, between the ADP-bound and ATP-analogue-bound states. The vital role of α4 has been further emphasised by a 3D image of Kar3 in the tightly bound empty state, where it appears to melt on to the MT surface. In this state, loop L7 also interacts closely with tubulin, distorting the central β-sheet, which may be important in controlling the binding site on the motor domain for the neck that connects to the cargo-binding region. Both of these changes were a surprise because no equivalent state has yet been seen by X-ray crystallography and this tightly bound state has not yet been observed at high resolution for another type of motor domain.

In addition to the need for supporting images of the tightly-bound empty state, there remain many questions about the sequence of changes in tubulin-bound motor domains when ATP binds and is hydrolysed. The movement observed for helix α6, that also seems to connect the nucleotide-binding and neck regions, is intriguing and needs to be compared in more detail for plus-end-directed and minus-end-directed motors. Ideally, it would be desirable to crystallise kinesin-tubulin complexes and view the interfaces between the proteins in different states at near-atomic resolution. Failing this, there remains the hope of pushing the resolution of the EM images much higher, perhaps to 4 Å or better. The specimens used in the work reviewed here did not appear to be limiting the resolution obtainable. The number of images required to see detail at higher resolution will grow steeply but, fortunately, the human effort involved will be reduced by recently developed computer programs. In particular, being able to analyse images of 13- or 14-protofilament MTs (Li et al., 2001; Kikkawa, 2004; Sindelar and Downing, 2007) will help in data collection. Previous use of the rare 15-protofilament tubes, which are perfectly helical and therefore easier to analyse, meant that only a small fraction of the images recorded were used. In future it should be possible to use the majority of images.

## References


**Al-Bassam, J., Cui, Y., Klopfenstein, D., Carragher, B. O., Vale, R. D. and Milligan, R. A.** (2003). Distinct conformations of the kinesin Unc104 neck regulate a monomer to dimer motor transition. *J. Cell Biol.* **163**, 743-753.

**Alonso, M. C., Vanderkerckhove, J. and Cross, R. A.** (1998). Proteolytic mapping of kinesin/ncd-microtubule interface: Nucleotide-dependent conformational changes in the loops L8 and L12. *EMBO J.* **17**, 945-951.

**Alonso, M. C., Drummond, D. R., Kain, S., Hoeng, J., Amos, L. A. and Cross, R. A.** (2007). An ATP gate controls tubulin binding by the tethered head of kinesin-1. *Science* **316**, 120-123.

**Arnal, I. and Wade, R. H.** (1998). Nucleotide-dependent conformations of the kinesin dimer interacting with microtubules. *Structure* **6**, 33-38.

**Carter, N. J. and Cross, R. A.** (2005). Mechanics of the kinesin step. *Nature* **435**, 308-312.

**Cohn, S. A., Ingold, A. L. and Scholey, J. M.** (1989). Quantitative analysis of sea urchin egg kinesin-driven microtubule motility. *J. Biol. Chem.* **264**, 4290-4297.

**Cross, R. A., Crevel, I., Carter, N. J., Alonso, M. C., Hirose, K. and Amos, L. A.** (2000). The conformational cycle of kinesin. *Philos. Trans. R. Soc. Lond. B Biol. Sci.* **355**, 459-464.

**Endres, N. F., Yoshioka, C., Milligan, R. A. and Vale, R. D.** (2006). A lever-arm rotation drives motility of the minus-end-directed kinesin Ncd. *Nature* **439**, 875-878.

**Hackney, D. D.** (2007). Processive motor movement. *Science* **316**, 58-59.

**Hancock, W. O. and Howard, J.** (1998). Processivity of the motor protein kinesin requires two heads. *J. Cell Biol.* **140**, 1395-1405.

**Hirose, K., Lockhart, A., Cross, R. A. and Amos, L. A.** (1996). Three-dimensional cryoelectron microscopy of dimeric kinesin and ncd motor domains on microtubules. *Proc. Natl. Acad. Sci. USA* **93**, 9539-9544.

**Hirose, K., Cross, R. A. and Amos, L. A.** (1998). Nucleotide-dependent structural changes in dimeric NCD molecules complexed to microtubules. *J. Mol. Biol.* **278**, 389-400.

**Hirose, K., Löwe, J., Alonso, M., Cross, R. A. and Amos, L. A.** (1999). Congruent docking of dimeric kinesin and ncd into three-dimensional electron cryomicroscopy maps of microtubule-motor ADP complexes. *Mol. Biol. Cell* **10**, 2063-2074.

**Hirose, K., Akimaru, E., Akiba, T., Endow, S. A. and Amos, L. A.** (2006). Large conformational changes in a kinesin motor catalysed by interaction with microtubules. *Mol. Cell* **23**, 913-923.

**Hoenger, A., Sack, S., Thormahlen, M., Marx, A., Muller, J., Gross, H. and Mandelkow, E.** (1998). Image reconstructions of microtubules decorated with monomeric and dimeric kinesins: comparison with X-ray structure and implications for motility. *J. Cell Biol.* **141**, 419-430.

**Hoenger, A., Thormahlen, M., Diaz-Avalos, R., Doerhoefer, M., Goldie, K. N., Muller, J. and Mandelkow, E.** (2000). A new look at the microtubule binding patterns of dimeric kinesins. *J. Mol. Biol.* **297**, 1087-1103.

**Kikkawa, M.** (2004). A new theory and algorithm for reconstructing helical structures with a seam. *J. Mol. Biol.* **343**, 943-955.

**Kikkawa, M. and Hirokawa, N.** (2006). High-resolution cryo-EM maps show the nucleotide binding pocket of KIF1A in open and closed conformations. *EMBO J.* **25**, 4187-4194.

**Kikkawa, M., Sablin, E. P., Okada, Y., Yajima, H., Fletterick, R. J. and Hirokawa, N.** (2001). Switch-based mechanism of kinesin motors. *Nature* **411**, 439-445.

**Klumpp, L. M., Hoenger, A. and Gilbert, S. P.** (2004). Kinesin's second step. *Proc. Natl. Acad. Sci. USA* **101**, 3444-3449.

**Kozielski, F., Sack, S., Marx, A., Thormahlen, M., Schonbrunn, E., Biou, V., Thompson, A., Mandelkow, E. M. and Mandelkow, E.** (1997). The crystal structure of dimeric kinesin and implications for microtubule-dependent motility. *Cell* **91**, 985-994.

**Kozielski, F., De Bonis, S., Burmeister, W. P., Cohen-Addad, C. and Wade, R. H.** (1999). The crystal structure of the minus-end-directed microtubule motor protein ncd reveals variable dimer conformations. *Structure* **7**, 1407-1416.

**Kull, F. J., Sablin, E. P., Lau, R., Fletterick, R. J. and Vale, R. D.** (1996). Crystal structure of the kinesin motor domain reveals a structural similarity to myosin. *Nature* **380**, 550-555.

**Li, H., DeRosier, D. J., Nicholson, W. V., Nogales, E. and Downing, K. H.** (2002). Microtubule structure at 8 A resolution. *Structure* **10**, 1317-1328.

**Löwe, J., Li, H., Downing, K. H. and Nogales, E.** (2001). Refined structure of alpha beta-tubulin at 3.5 A resolution. *J. Mol. Biol.* **313**, 1045-1057.

**Moores, C. A. and Milligan, R. A.** (2006). Lucky 13 – microtubule depolymerisation by kinesin-13 motors. *J. Cell Sci.* **119**, 3905-3913.

**Neumann, E., Garcia-Saez, I., DeBonis, S., Wade, R. H., Kozielski, F. and Conway, J. F.** (2006). Human kinetochore-associated kinesin CENP-E visualized at 17 A resolution bound to microtubules. *J. Mol. Biol.* **362**, 203-211.

**Nitta, R., Kikkawa, M., Okada, Y. and Hirokawa, N.** (2004). KIF1A alternately uses two loops to bind microtubules. *Science* **305**, 678-683.

**Ogawa, T., Nitta, R., Okada, Y. and Hirokawa, N.** (2004). A common mechanism for microtubule destabilizers – M type kinesins stabilize curling of the protofilament using the class-specific neck and loops. *Cell* **116**, 591-602.

**Rice, S., Lin, A. W., Safer, D., Hart, C. L., Naber, N., Carragher, B. O., Cain, S. M., Pechatnikova, E., Wilson-Kubalek, E. M., Whittaker, M. et al.** (1999). A structural change in the kinesin motor protein that drives motility. *Nature* **402**, 778-784.

**Sablin, E. P., Case, R. B., Dai, S. C., Hart, C. L., Ruby, A., Vale, R. D. and Fletterick, R. J.** (1998). Direction determination in the minus-end-directed kinesin motor ncd. *Nature* **395**, 813-816.

**Sack, S., Müller, J., Marx, A., Thormählen, M., Mandelkow, E. M., Brady, S. T. and Mandelkow, E.** (1997). X-ray structure of motor and neck domains from rat brain kinesin. *Biochemistry* **36**, 16155-16165.

**Schnitzer, M. J. and Block, S. M.** (1997). Kinesin hydrolyses one ATP per 8-nm step. *Nature* **388**, 386-390.

**Sindelar, C. V. and Downing, K. H.** (2007). The beginning of kinesin's force-generating cycle visualized at 9-A resolution. *J. Cell Biol.* **177**, 377-385.

**Sindelar, C. V., Budny, M. J., Rice, S., Naber, N., Fletterick, R. and Cooke, R.** (2002). Two conformations in the human kinesin power stroke defined by X-ray crystallography and EPR spectroscopy. *Nat. Struct. Biol.* **9**, 844-848.

**Sosa, H., Hoenger, A. and Milligan, R. A.** (1997). Three different approaches for calculating the three-dimensional structure of microtubules decorated with kinesin motor domains. *J. Struct. Biol.* **118**, 149-158.

**Turner, J., Anderson, R., Guo, J., Beraud, C., Fletterick, R. and Sakowicz, R.** (2001). Crystal structure of the mitotic spindle kinesin Eg5 reveals a novel conformation of the neck-linker. *J. Biol. Chem.* **276**, 25496-25502.

**Vale, R. D. and Milligan, R. A.** (2000). The way things move: looking under the hood of molecular motor proteins. *Science* **288**, 88-95.

**Vale, R. D., Funatsu, T., Pierce, D. W., Romberg, L., Harada, Y. and Yanagida, T.** (1996). Direct observation of single kinesin molecules moving along microtubules. *Nature* **380**, 451-453.

**Wendt, T. G., Volkmann, N., Skiniotis, G., Goldie, K. N., Muller, J., Mandelkow, E. and Hoenger, A.** (2002). Microscopic evidence for a minus-end-directed power stroke in the kinesin motor ncd. *EMBO J.* **21**, 5969-5978.

**Woehlke, G., Ruby, A. K., Hart, C. L., Ly, B., Hom-Booher, N. and Vale, R. D.** (1997). Microtubule interaction site of the kinesin motor. *Cell* **90**, 207-216.

**Young, E. C., Mahtani, H. K. and Gelles, J.** (1998). One-headed kinesin derivatives move by a nonprocessive, low-duty ratio mechanism unlike that of two-headed kinesin. *Biochemistry* **37**, 3467-3479.

**Yun, M., Zhang, X., Park, C. G., Park, H. W. and Endow, S. A.** (2001). A structural pathway for activation of the kinesin motor ATPase. *EMBO J.* **20**, 2611-2618.

**Yun, M., Bronner, C. E., Park, C. G., Cha, S. S., Park, H. W. and Endow, S. A.** (2003). Rotation of the stalk/neck and one head in a new crystal structure of the kinesin motor protein, Ncd. *EMBO J.* **22**, 5382-5389.